PHYSICAL REVIEW B, VOLUME 64, 184407

Spin and orbital magnetic moments of $3d$ and $4d$ impurities in and on the (001) surface of bcc Fe

V. Popescu and H. Ebert
Department Chemie/Physikalische Chemie, Universität München, Butenandtstr. 5-13, D-81377 München, Germany

B. Nonas and P. H. Dederichs
Institut für Festkörperforschung, Forschungszentrum Jülich, Postfach 1913, D-52425 Jülich, Germany

(Received 23 November 2000; revised manuscript received 3 May 2001; published 17 October 2001)

Results of *ab initio* calculations of the magnetic moments of $3d$ and $4d$ transition metal impurities in and on the (001) surface of bcc Fe are presented. These investigations were performed using the spin-polarized relativistic version of the Korringa-Kohn-Rostoker Green's-function method giving access to the spin as well as the orbital magnetic moments induced by spin-orbit coupling. For the spin magnetic moment only small changes are found compared to a previous scalar-relativistic calculation for the investigated surface impurity systems. In most cases the orbital magnetic moment turned out to be somewhat enlarged compared to that of the impurity dissolved in bulk Fe. A rather simple explanation for the variation of these spin-orbit-induced moments with atomic number of the impurity atom could be given on the basis of perturbation theory.

DOI: 10.1103/PhysRevB.64.184407 PACS number(s): 75.20.Hr, 61.72.Ss

I. INTRODUCTION

Recently, the magnetic properties of surfaces have received a lot of interest. One of the most prominent features found in this field is the enhancement of the spin magnetism at the surface for spontaneously spin-polarized systems.[1–6] Closely related to this is the prediction that certain surface layer systems built up by normally nonmagnetic components create a spontaneous spin magnetization due to the reduced coordination at the surface.[4,7]

Another important aspect of surface magnetism is the influence of the spin-orbit coupling. A very impressive example for this is the creation of a spin-polarized photocurrent from a (111) surface of paramagnetic Pt using linearly polarized light. For spontaneously magnetized systems, the magneto-optical Kerr effect (MOKE) supplies an important example for spin-orbit-induced phenomena.[8] While being in most cases primarily a bulk property, there are also some surface specific features concerning the MOKE.[9–11] This applies even more to the magnetocrystalline anisotropy for which now quite reliable calculations can be performed in the case of transition metal multilayers and surface layer systems.[12,13] Closely related to contribution to the magnetocrystalline anisotropy due to the spin-orbit coupling is the occurrence of an orbital magnetic moment. Quite similar to the case of the spin magnetic moment an enhancement of this spin-orbit-induced contribution to the total magnetic moment has been found for surface layer systems.[4–6]

In this contribution results of fully relativistic calculations of the magnetic properties for $3d$ and $4d$ impurities in and on the surface layer of a (001) surface of bcc Fe are presented. The computational scheme that has been used for this purpose is sketched shortly in the next section. The main part of the paper is devoted to the discussion of the corresponding results. Concerning this, the influence of the specific atomic configuration on the spin and orbital magnetic moments will be of particular interest. For the latter one a simple model will be used to give a semiquantitative description of this purely relativistic property.

II. COMPUTATIONAL ASPECTS

The work presented here was performed on the basis of density functional theory using a local spin density approximation (LSDA) for exchange and correlation. Within this framework the electronic structure of the investigated systems was described in terms of the corresponding electronic Green's function. This in turn was evaluated by means of multiple-scattering theory. For the nonrelativistic case this approach is described in some detail in Ref. 14. With the Green's function available, the electronic structure of a substitutional impurity can be described straightforwardly by means of the Dyson equation. Due to the angular momentum representation used for the Green's function, the Dyson equation in real space can be transformed to an equivalent algebraic matrix equation. The dimension of the matrices occurring in that equation is fixed by the cutoff l_{max} of the angular momentum expansion and the number of host atoms around the impurity atom that are assumed to be disturbed by the impurity. This scheme has been applied recently for the scalar-relativistic case to study the spin magnetic properties of $3d$ and $4d$ transition metal impurities in and on the (001) surface of bcc Fe and fcc Ni.[15,16]

In the following it is assumed that the impurity atom replaces substitutionally an Fe atom in the surface layer or occupies a regular lattice site in the vacuum region next to the Fe surface layer (adatom position). The corresponding calculations have been performed by accounting for a perturbation of the host atomic potentials within two atomic neighboring shells around the impurity atom. The convergence of Green's function calculations with respect to the size of the perturbed-potential cluster has been investigated in detail by Stefanou *et al.*[17] In a fcc crystal the moment of a magnetic impurity is typically converged up to $10^{-2}\mu_B$ if the potentials of the nearest neighbors are included in the self-consistency procedure. In a bcc crystal the same accuracy is achieved if the first two shells are included, which is due to the nearly equal distances to these two shells. At the surface the convergence of impurity calculations is very similar to

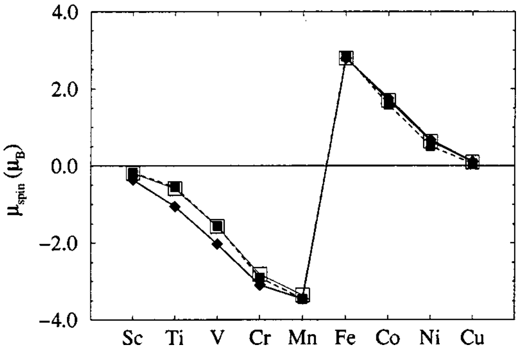

FIG. 1. Spin magnetic moment μ_{spin} of $3d$ transition metal impurity atoms at the (001) surface of bcc Fe sitting in and on the surface layer (in, solid squares; on, solid diamonds). In addition the results of the corresponding scalar-relativistic calculations for the in position are given by open squares.

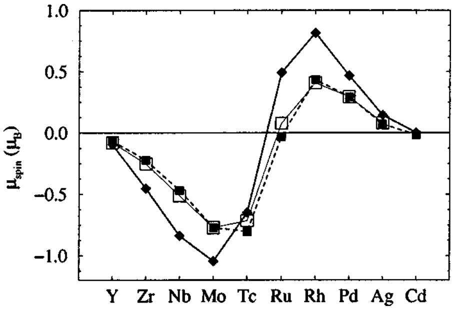

FIG. 2. The same as Fig. 1 but for $4d$ transition metal atoms.

the bulk, as has been found in test calculations with much larger clusters.[18] In the present calculations the perturbed cluster contained in fact 19 potentials: the impurity, all first and second neighbors, and four more sites in the layer of the impurity. For the self-consistency cycle the parametrization for the exchange and correlation potential proposed by Vosko *et al.*[19] has been used.

To study the influence of the spin-orbit coupling on the magnetic properties of the impurity systems considered, we used for the present work a fully relativistic version of the scheme described above. This means in particular that all calculations have been done in the framework of relativistic spin-density functional theory[20,21] (SDFT) (see discussion below). However, the corresponding Kohn-Sham-Dirac equations have not been solved self-consistently but the spin-dependent potential has been taken from the preceding scalar-relativistic calculation. For the systems studied here, this is not a serious approximation. This is obvious from the experience gained with corresponding calculations for $3d$ and $4d$ transition metal alloys where the self-consistency cycle including all relativistic effects changed the spin and orbital magnetic moments only by some few percents compared to a non-self-consistent calculation using potential sets created in a non- or scalar-relativistic way.

The accuracy of non-self-consistent fully relativistic calculations with scalar-relativistic input potentials has also been recently studied in detail for $3d$, $4d$, and $5d$ adatoms on the surface of Ag and Au.[22] For the $3d$ as well as for the $4d$ adatoms the spin moments are practically not affected by the spin-orbit coupling (as can be seen in Figs. 1 and 2) or by the "new" self-consistency iterations. In the $3d$ series both procedures give the same spin moments with an accuracy of better than $10^{-2}\mu_B$. For the $4d$ adatoms the deviations are somewhat larger, but well below $10^{-1}\mu_B$. Significant deviations are obtained only for $5d$ impurities being due to the much larger spin-orbit coupling constant. These impurities, however, are not considered in the present paper.

Within the spin-polarized relativistic version of the Koringa-Kohn-Rostoker (KKR) formalism the Green's function may be written as[23]

$$\begin{aligned} G^+(\vec{r}_n,\vec{r}\,'_m,E) = & \sum_{\Lambda\Lambda'} Z_\Lambda(\vec{r}_n,E)\,\tau^{nm}_{\Lambda\Lambda'}(E)\,Z^\times_{\Lambda'}(\vec{r}\,'_m,E) \\ & -\sum_{\Lambda}\,[Z_\Lambda(\vec{r}_n,E)J^\times_\Lambda(\vec{r}\,'_n,E)\Theta(r'_n-r_n) \\ & +J_\Lambda(\vec{r}_n,E)Z^\times_\Lambda(\vec{r}\,'_n,E)\Theta(r_n-r'_n)]\delta_{nm}. \end{aligned} \tag{1}$$

Here we adopted a notation analogous to the nonrelativistic counterpart introduced by Faulkner and Stocks.[24] Z and J are the regular and irregular solutions to the Dirac equation for a spin-polarized single-site potential well. Accordingly, these functions are labeled by the relativistic spin-orbit and magnetic quantum numbers $\Lambda=(\kappa,\mu)$.[25] Of course, the expression for the Green's function given in Eq. (1) is completely equivalent to that used in Ref. 15. This means in particular that the scattering path operator $\tau^{nm}_{\Lambda\Lambda'}(E)$ carries the same information on the multiple-scattering events in the system as the structural Green's function used in Ref. 15 (the explicit expression connecting both conventions is given for example by Zeller *et al.*[26]). Finally it should be noted that Eq. (1) is dealt with using the atomic sphere approximation (ASA) as was done in the previous work.[15]

The larger error of the ASA in surface calculations does not arise from the spherical approximation for the potential but from the additional spherical approximation for the charge density. Reliable surface energies, for instance, can be obtained only if the dipolar charge contributions are included in the Coulomb energies.[27,28] Note that in the present calculations the full charge density is included, so that the ASA is only used for the potential. The additional, rather modest, improvements of a full-potential treatment concern mostly the charge distribution in the vacuum.[29] The effect on the local moments, around $10^{-2}\mu_B$, and on the density of states (DOS) are very small. For the clean Fe (001) surface we obtained a charge of 0.50 electrons in the first and 0.05 electrons in the second vacuum layers. For the Ni (001) surface these numbers are 0.31 and 0.01 electrons, respectively.

Within the scalar-relativistic scheme sketched above the surface is treated as the boundary of a half-infinite solid. For the corresponding calculations it was assumed that the fifth Fe layer counted inward starting from the surface layer is already identical to Fe bulk. The same was assumed for the other direction, i.e., towards the vacuum region. For the fully relativistic calculations we represent the surface region by a finite cluster of potential wells (note that the vacuum region is accounted for by so-called empty spheres centered on regular lattice sites). For all calculations a cluster of 13 shells around the impurity atom, containing 259 atoms in total, has been used. For this big cluster size the resulting moments are reasonably converged; i.e., the uncertainty of the spin and orbital magnetic moments is smaller than 5% and 10%, respectively.[30]

The adopted cluster approach allows to obtain the scattering path operator in Eq. (1) by simply inverting the real-space KKR matrix:[31]

$$\underline{\underline{M}}(E)=\underline{\underline{m}}(E)-\underline{\underline{G}}(E). \tag{2}$$

Here $\underline{\underline{m}}$ is a matrix diagonal with respect to the site indices n and with its elements given by the inverse of the single-site scattering matrices $\underline{\underline{t}}$ [with $(\underline{\underline{t}})^n=\underline{t}^n$] corresponding to the potential centered at site n. The quantity $\underline{\underline{G}}$ is the so-called real-space KKR structure constant matrix describing the propagation of free electrons with energy E. Finally, $\underline{\tau}^{nm}$ is given by $(\underline{\underline{M}}^{-1})^{nm}$. With the Green's function available the spin and orbital magnetic moments are obtained from[23]

$$\mu_{spin}=-\frac{\mu_B}{\pi}\mathrm{Im\,Tr}\int^{E_F}dE\int d^3r\beta\sigma_z G^+(\vec{r},\vec{r},E), \tag{3}$$

$$\mu_{orb}=-\frac{\mu_B}{\pi}\mathrm{Im\,Tr}\int^{E_F}dE\int d^3r\beta l_z G^+(\vec{r},\vec{r},E). \tag{4}$$

Here E_F is the Fermi energy, which has been determined from a separate calculation for the bulk.

III. RESULTS AND DISCUSSION

A. Properties of the unperturbed Fe surface

As a first application of the cluster approach described above the unperturbed (001) surface of bcc Fe has been investigated. The resulting spin magnetic moments μ_{spin} for the Fe layers close to the surface $[(2.99,2.16,2.28,2.27,2.28)\mu_B$ starting from the surface layer with the last value corresponding to bulk Fe] are in fair agreement with the results of the preceding scalar-relativistic calculation $[(2.79,2.05,2.13,2.04,2.09)\mu_B]$. These data show the well-known enhancement of μ_{spin} at the surface.[1–6] The common explanation for this is the reduced coordination number at the surface leading to a decrease in the *d*-band width that is accompanied by an increase of the paramagnetic DOS $n(E_F)$ at the Fermi energy. According to the Stoner criterion this increases locally the tendency for the spontaneous formation of a spin magnetic moment. For a more detailed explanation one observes that the majority *d* band of Fe, being only partially filled in the bulk, becomes—as a result of the band narrowing—completely filled at the surface. Since the total *d* charge of the surface atoms is more or less conserved, the number of occupied minority states decreases by the same amount, so that as a result the moment at the surface increases.

A similar behavior is also found for the spin-orbit-induced orbital magnetic moment μ_{orb} $[(0.081,0.057,0.043,0.044,0.057)\mu_B]$ for which the enhancement at the surface is even more pronounced than for μ_{spin}. Very similar results have been obtained for example for Fe $[(0.12,0.06,0.05,0.05)\mu_B]$, Co $[(0.11,0.09,0.09)\mu_B]$, and Ni $[(0.06,0.05,0.04,0.04)\mu_B]$ by Eriksson *et al.*[5,7] as well as Hjortstam *et al.*[6] using slab-type calculations. The later authors give three possible sources for the enhancement of μ_{orb} at the surface: (i) the *d*-band width decreases, leading to the filling of the majority band (see above). The contribution to μ_{orb} coming from a nearly filled band, however, is very small. For that reason the contribution to μ_{orb} from minority states becomes dominant, causing μ_{orb} to increase in this way. (ii) The reduced symmetry at the surface. (iii) The DOS $n(E_F)$ at E_F is enhanced. Of course these mechanisms are intimately interwoven and difficult to separate. For that reason a model will be used below that accounts for all of them at the same time.

B. Spin magnetic moments of 3*d* and 4*d* impurities at the (001) surface of bcc Fe

Adding impurities at the Fe surface or embedding them in the surface layer gives rise, of course, to a change of the magnetic moments of the surrounding Fe atoms. Concerning the spin magnetic moments, these are most pronounced and negative for the early elements of a transition metal row. For the late elements, on the other hand, the changes are much smaller. In addition, the influence of the impurity drops very rapidly with the distance; in general, the change of the moment is less than half for the next-nearest Fe atoms as compared to the nearest neighbors. A more detailed discussion of this issue can be found in Ref. 18.

The corresponding results of our cluster calculations for μ_{spin} of 3*d* and 4*d* transition metal impurities in and on the (001) surface of Fe are given in Figs. 1 and 2, respectively. In both figures the results of the previous scalar-relativistic calculation for the in-surface position have been added. A comparison with the fully relativistic cluster data demonstrate that—as stated above—the latter data are well converged with respect to the size of the cluster. In addition, one notices that inclusion of relativistic effects has not much impact on the spin magnetic moments.

For all sets of calculations an antiferromagnetic alignment of the spin magnetic moment is found for the early transition metals, while the late ones show a ferromagnetic coupling to the Fe host. This behavior is analogous to that known for the impurities dissolved in bulk Fe. The origin of the S-like curve shown in Figs. 1 and 2 is essentially the variation of the atomic energy level of the *d* states with respect to those of the Fe host, being exchange split. This mechanism has been discussed in great detail for the corresponding bulk systems in the past on the basis of tight binding[32,33] as well as *ab initio* calculations.[34] In addition, the difference of the 4*d* impurity spin magnetic moment for the bulk as well as the in- and on-surface positions (see Fig. 2) has been discussed by Nonas *et al.*[15] and traced back to a difference in hybridization with an Fe surface state close to the Fermi level. With this in mind it seems at first sight astonishing that for the 3*d*

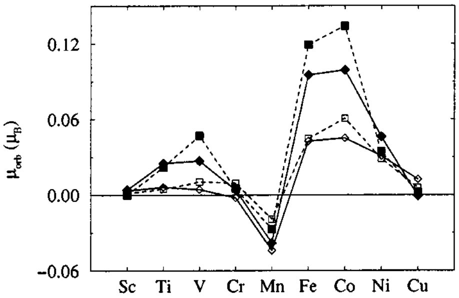

FIG. 3. Spin-orbit-induced orbital magnetic moment μ_{orb} of 3d transition metal impurity atoms at the (001) surface of bcc Fe sitting in and on the surface layer (in, solid squares; on, solid diamonds). In addition the results obtained from the estimation based on Eq. (5) are given by open symbols.

impurities there is not much difference in μ_{spin} for the in- and on-surface positions (see Fig. 1).

The reason for this seems to be partly that the spin magnetic moment of the 3d impurities is nearly saturated; i.e., the d band is nearly fully spin polarized. Partly this is also a peculiarity of the bcc (001) surface, which has the same number of nearest neighbors for the adatom as well as the surface atom position. Due to the shorter extend of the 3d wave functions, the 3d impurities have for both positions nearly the same moments. On the other hand, significant deviations occur for 4d impurities. In this case, due to a larger extend of the 4d wave function, the number of second nearest neighbors becomes important: for the bcc structure there are 5 for the surface layer position, but only 1 for the adatom position. Therefore, the 4d elements have considerably larger moments as adatoms as compared to atoms in the surface layer, whereas for 3d atoms both values are nearly the same. For Rh, it is often that an extraordinary behavior is found. However, the special role of Rh exists only in systems where Rh-Rh hybridization dominates the behavior, e.g., Rh clusters in free space or on noble metal surfaces. On the surface of Fe, the Rh hybridization with Fe is extremely strong, so that the behavior of a single Rh atom is quite normal.

C. Orbital magnetic moments of 3d and 4d impurities at the (001) surface of bcc Fe

The results for μ_{orb} of the investigated impurity systems obtained by the relativistic cluster calculations are shown in Figs. 3 and 4. The main features of these data sets are the same: for the beginning and the end of the series one has a positive orbital magnetic moment. In the middle of the series there is a dip in the curve with partly negative moments. This dip is more pronounced for the 4d elements than for the 3d elements and shifted to higher atomic numbers. This finding is in full line with previous results for 5d impurities dissolved in bcc Fe.[35] In that case the biggest spin-orbit-induced orbital magnetic moment was found for Ir with antiparallel orientation to the host spin magnetization.

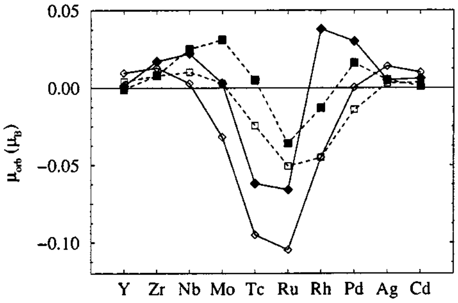

FIG. 4. The same as Fig. 3 but for 4d transition metal atoms.

Quite similar to the result for μ_{spin} of the 3d elements it is found that μ_{orb} does not depend very much on the specific position of the impurity atom. This seems to indicate that the behavior of μ_{orb} is connected to that of μ_{spin} according to mechanism (i) mentioned above (change of the occupation of the spin-up and -down states).

For the 4d elements a much stronger dependence of the orbital magnetic moment on the position is found. This behavior again goes parallel with that of μ_{spin}. In particular one notes that all the main features of the μ_{orb} curve—i.e., extrema and zeros—are shifted to lower atomic numbers when going from the in to the on position—just as was found for μ_{spin} (see Fig. 2).

To get more insight into the mechanism giving rise to μ_{orb}, estimations have been made based on the following expression:[35]

$$\langle l_z \rangle = -\sum_{lm_lm_s} \xi_l m_l^2 m_s n_{lm_lm_s}(E_F), \tag{5}$$

where ξ_l is the spin-orbit coupling parameter defined by[36]

$$\xi_l = \frac{1}{c^2}\int_0^{R_{max}} r R_l^2(r)\frac{dV(r)}{dr}dr, \tag{6}$$

where $R_l(r)$ is the radial wave function for the angular momentum l.

To arrive at this equation one starts from a non- or scalar-relativistic calculation giving the l-, m_l-, and m_s-resolved DOS $n_{lm_lm_s}$. To account for the perturbation due to spin-orbit coupling the term $\xi\vec{l}\cdot\vec{s}$ can be restricted to its part $\xi l_z \cdot s_z$ because the perturbation is treated in first order.[37] Accordingly, the resulting nonvanishing expectation value $\langle l_z \rangle$ is first order with respect to ξ_l. Because of this, $\langle l_z \rangle$ is primarily connected with a reoccupation of the states in the vicinity of the Fermi level. This leads to Eq. (5) from which the orbital magnetic moment is obtained via the expression $\mu_{orb} = \langle l_z \rangle \mu_B$. For the systems studied here it is of course sufficient to restrict the sum in Eq. (5) to $l=2$, i.e., to d electrons. The corresponding spin-orbit coupling parameter ξ_d is given in Fig. 5 for the Fermi energy. As expected, the values are smaller for the 3d elements than for the 4d elements. In both cases one notes an increase of ξ_d with increasing atomic number because the corresponding wave function gets more contracted by the increasingly attractive potential in the nuclear-near region. In addition, one may note that the values for ξ_d are all increased by around 10% compared to the free-atom values given by Koelling and MacDonald[38]

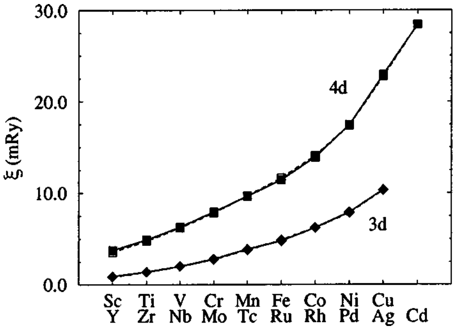

FIG. 5. The spin-orbit coupling parameter ξ_d for the *d* states of 3*d* and 4*d* transition metal impurities in and on the (001) surface of bcc Fe calculated for the Fermi energy. The results for both positions are practically identical.

because the potential is more attractive for the solid state and because the wave function is normalized within the Wigner-Seitz sphere.

The orbital magnetic moments estimated on the basis of Eq. (5) and the data for ξ_d shown in Fig. 5 have been added in Figs. 3 and 4. For the 3*d* elements the simple model is obviously able to give a semiquantitative account of the rigorously calculated results based on Eq. (4). In particular, one can conclude that the spin-orbit-induced orbital magnetic moment for the 3*d* elements is of the same order of magnitude as for the 4*d* elements—although the corresponding spin-orbit coupling parameter ξ_d is about a factor of 2 smaller—because the corresponding DOS related term is higher. This can be seen as a consequence of the smaller *d*-band width of the 3*d* element compared to that of the 4*d* elements.

On the basis of Eq. (5) the variation of μ_{orb} along the 3*d* row can be explained in a simple way. For the early elements Sc, Ti, V, and Cr on or in the surface layer, the majority *d* band is empty due to the antiferromagnetic coupling with the Fe host. Accordingly, the filling of the minority band determines $n_{m_l}(E_F)$ and with that the orbital moment. In particular, μ_{orb} turns out to be positive for that reason. For the late transition metals Fe, Co, and Ni, on the other hand, the majority band is filled. For this reason, only the minority band determines μ_{orb}, which again has to be positive. For Mn, the situation is more complex because both bands are not completely filled. This leads in particular to the dip in the curve in Fig. 4, with a negative orbital moment.

Application of Eq. (5) for the 4*d* elements results in the middle of the series in values for μ_{orb} that by far overshoot the rigorously calculated results. Nevertheless, one notes that the trend of μ_{orb} along the series is properly reproduced by the estimation. Similar to the 3*d* elements, the majority band of the early 4*d* elements Zr and Nb is empty, leading to a positive orbital magnetic moment, while for the late elements the majority band is filled, also giving rise to a positive μ_{orb}. In contrast to the 3*d* elements, the situation is much more complex in the middle of the 4*d* series. Nevertheless, the shift for the main features of the μ_{orb} curve when going from the in to the on position is accounted for by the model. For the on-surface position a strong peak in the majority-spin DOS at the Fermi energy E_F occurs for Tc and Ru, leading to a relatively large negative orbital moment. For the in-surface position, on the other hand, a larger majority peak at E_F is present only for Ru while a smaller majority peak occurs for Rh.

Concerning the difference of the orbital moments based on Eq. (5) with the properly calculated ones using the fully relativistic approach together with Eq. (4), one has to emphasize that Eq. (5) is based on a number of simplifications. Obviously, these are here more problematic for the 4*d* than for the 3*d* elements. A way to improve the quantitative agreement would be to drop these simplifications and to perform a full perturbational calculation, following essentially the lines of the approach suggested by Solovyev *et al.* in Ref. 36. However, this would not lead to the very transparent picture based on Eq. (5).

On the basis of these findings, one can conclude that the spin-orbit-induced orbital magnetic moment for all the impurity systems studied here can be traced back to the variation of n_{lm_lms} with the atomic number and the spatial atomic position. This in turn is primarily determined by the relative position of the atomic energy levels of the *d*-like states with respect to the corresponding exchange-split levels of Fe, the *d*-band width, and the coordination number.

In total, the orbital moments of the 3*d* and 4*d* impurities in and on the Fe surface are of about the same size as the bulk or surface orbital moments of Fe, Co, and Ni. Thus, even a single adatom on the Fe(001) surface behaves in this respect rather bulk like with a nearly quenched orbital moment and is far away from the behavior of free atoms, the orbital moments of which are determined by Hund's second rule.

IV. SUMMARY

We have presented a study of the magnetic properties of 3*d* and 4*d* transition metal impurities at the (001) surface of bcc Fe. The fully relativistic calculations revealed that the spin magnetic moment of the impurity atoms is not much affected by the inclusion of relativistic effects. On the other hand, accounting for the spin-orbit coupling resulted in quite pronounced orbital magnetic moments. The dependence of these with the position of the impurity atom at the surface and in the periodic table could be described by a rather simple model based on perturbation theory. Apart from the spin-orbit coupling parameter ξ the central quantity of this model is the m_l- and m_s-resolved DOS $n_{lm_lm_s}$ of the *d* electrons at the Fermi level. The latter quantity is of course highly sensitive to the specific details of the hybridization of impurity states with those of the Fe host.

ACKNOWLEDGMENT

This work was supported by the Deutsche Forschungsgemeinschaft (DFG) within the program "Theorie relativistischer Effekte in der Chemie und Physik schwerer Elemente."

[1] D. Wang, A.J. Freeman, and H. Krakauer, Phys. Rev. B **26**, 1340 (1982).

[2] O. Jepsen, J. Madsen, and O.K. Andersen, Phys. Rev. B **26**, 2790 (1982).

[3] E. Wimmer, A.J. Freeman, and H. Krakauer, Phys. Rev. B **30**, 3113 (1984).

[4] O. Eriksson, G.W. Fernando, A.M. Boring, and R.C. Albers, Solid State Commun. **78**, 801 (1991).

[5] O. Eriksson *et al.*, Phys. Rev. B **45**, 2868 (1992).

[6] O. Hjortstam *et al.*, Phys. Rev. B **53**, 9204 (1996).

[7] O. Eriksson, R.C. Albers, and A.M. Boring, Phys. Rev. Lett. **66**, 1350 (1991).

[8] H. Ebert, in *Spin-orbit Influenced Spectroscopies of Magnetic Solids*, Vol. 466 of *Lecture Notes in Physics*, edited by H. Ebert and G. Schütz (Springer, Berlin, 1996), p. 159.

[9] S.D. Bader, J. Magn. Magn. Mater. **100**, 440 (1991).

[10] Y. Suzuki *et al.*, Phys. Rev. Lett. **68**, 3355 (1992).

[11] Y. Suzuki *et al.*, J. Magn. Magn. Mater. **121**, 539 (1993).

[12] G.Y. Guo, H. Ebert, and W.M. Temmerman, J. Phys.: Condens. Matter **3**, 8205 (1991).

[13] B. Újfalussy, L. Szunyogh, P. Bruno, and P. Weinberger, Phys. Rev. Lett. **77**, 1805 (1996).

[14] R. Zeller, P. Lang, B. Drittler, and P.H. Dederichs, in *Application of Multiple Scattering Theory*, edited by W. H. Butler *et al.*, Mater. Res. Soc. Symp. Proc. No. 253 (Materials Research Society, Pittsburgh, 1992), p. 357.

[15] B. Nonas, K. Wildberger, R. Zeller, and P.H. Dederichs, Phys. Rev. B **57**, 84 (1998).

[16] B. Nonas, K. Wildberger, R. Zeller, and P.H. Dederichs, J. Magn. Magn. Mater. **165**, 137 (1997).

[17] N. Stefanou, A. Oswald, R. Zeller, and P.H. Dederichs, Phys. Rev. B **35**, 6911 (1987).

[18] B. Nonas, Master's thesis, Technical University Aachen, 1996.

[19] S.H. Vosko, L. Wilk, and M. Nusair, Can. J. Phys. **58**, 1200 (1980).

[20] A.H. MacDonald and S.H. Vosko, J. Phys. C **12**, 2977 (1979).

[21] M.V. Ramana and A.K. Rajagopal, J. Phys. C **12**, L845 (1979).

[22] B. Nonas, Ph.D. thesis, Technical University Aachen, 2000.

[23] H. Ebert, P. Strange, and B.L. Gyorffy, J. Phys. F **18**, L135 (1988).

[24] J.S. Faulkner and G.M. Stocks, Phys. Rev. B **21**, 3222 (1980).

[25] M. E. Rose, *Relativistic Electron Theory* (Wiley, New York, 1961).

[26] R. Zeller *et al.*, Phys. Rev. B **52**, 8807 (1995).

[27] M. Alden *et al.*, Phys. Rev. B **46**, 6303 (1992).

[28] H.L. Skriver and N.M. Rosengaard, Phys. Rev. B **46**, 7157 (1992).

[29] N. Papanikolaou *et al.*, Phys. Rev. B **62**, 11 118 (2000).

[30] S.V. Beiden *et al.*, Phys. Rev. B **57**, 14 247 (1998).

[31] H. Ebert, V. Popescu, and D. Ahlers, Phys. Rev. B **60**, 7156 (1999).

[32] J. Kanamori, J. Appl. Phys. **36**, 929 (1965).

[33] I.A. Campbell and A.A. Gomez, Proc. Phys. Soc. London **91**, 319 (1967).

[34] R. Zeller, J. Phys. F **17**, 2123 (1987).

[35] H. Ebert, R. Zeller, B. Drittler, and P.H. Dederichs, J. Appl. Phys. **67**, 4576 (1990).

[36] I.V. Solovyev, P.H. Dederichs, and I. Mertig, Phys. Rev. B **52**, 13 419 (1995).

[37] H. Ebert, H. Freyer, and M. Deng, Phys. Rev. B **56**, 9454 (1997).

[38] D. D. Koelling and A. H. MacDonald, in *Relativistic Effects in Atoms, Molecules and Solids*, edited by G.L. Malli (Plenum Press, New York, 1979), p. 227.